ARTICLES

Journal of Semiconductors
(2019) 40, 062002
doi: 10.1088/1674-4926/40/6/062002

Comparison of tunneling currents in graphene nanoribbon tunnel field effect transistors calculated using Dirac-like equation and Schrödinger's equation

Endi Suhendi[1, †], Lilik Hasanah[1], Dadi Rusdiana[1], Fatimah A. Noor[2], Neny Kurniasih[3], and Khairurrijal[2]

[1]Physics of Electronic Material Research Division, Universitas Pendidikan Indonesia, Bandung 40154, Indonesia

[2]Physics of Electronic Material Research Division, Institut Teknologi Bandung, Bandung 40132, Indonesia

[3]Earth Physics and Physics of Complex Systems Research Division, Institut Teknologi Bandung, Bandung 40132, Indonesia

Abstract: The tunneling current in a graphene nanoribbon tunnel field effect transistor (GNR-TFET) has been quantum mechanically modeled. The tunneling current in the GNR-TFET was compared based on calculations of the Dirac-like equation and Schrödinger's equation. To calculate the electron transmittance, a numerical approach-namely the transfer matrix method (TMM)-was employed and the Launder formula was used to compute the tunneling current. The results suggest that the tunneling currents that were calculated using both equations have similar characteristics for the same parameters, even though they have different values. The tunneling currents that were calculated by applying the Dirac-like equation were lower than those calculated using Schrödinger's equation.

Key words: graphene nanoribbon; tunnel field effect transistor; tunneling current; Schrödinger equation; Dirac-like equation

Citation: E Suhendi, L Hasanah, D Rusdiana, F A Noor, N Kurniasih, and Khairurrijal, Comparison of tunneling currents in graphene nanoribbon tunnel field effect transistors calculated using Dirac-like equation and Schrödinger's equation[J]. *J. Semicond.*, 2019, 40(6), 062002. http://doi.org/10.1088/1674-4926/40/6/062002

1. Introduction

Following the synthesis of graphene, nanoelectronics have become a popular research topic. Many theoretical and experimental studies have been carried out and graphene is anticipated to be a prospective material to substitute silicon. Graphene, which is a two-dimensional material that consists of carbon atoms that forms a hexagonal lattice, has some very interesting electronic properties, such as zero band gap (semimetal), high carrier mobility[1], and long phase coherence length[2]. The band structure of graphene can be changed by setting a limit to its size. Graphene with a width smaller than its length is known as a graphene nanoribbon (GNR), and it can be used in one-dimensional electronic systems[3, 4]. Based on the edge shape, there are two types of GNRs: armchair graphene nanoribbons (AGNRs) and zigzag graphene nanoribbons (ZGNRs). AGNRs can be either semi-conductive or metallic in terms of their widths[5, 6], whereas the ZGNRs have metallic properties for all widths. GNRs can be used for various nanoelectronic devices using these properties, such as field-effect transistors (FET) and p–n junction diode. In a p–n junction diode, GNRs can be p- or n-type by doping[7] or electrostatically engineering[8]. In FET, GNRs can be used as a source, drain, and channel that connect the source and the drain.

Previous studies have modeled and simulated nanoelectronic device characteristics based on GNRs material. The Dirac-like equation and the Schrödinger equation are used to explain the behavior of an electron in this material. For a low energy limit, dispersion relation of electron and hole is linear and the effective electron mass is zero. Consequently, the system can be described through the Dirac-like equation[9]. This equation has been used to describe the traits of electronic devices, such as GNR p–n junction[10–12], GNR p–n–p bipolar junction[13, 14] and graphene FET for high-frequency application[15]. The Schrödinger equation can still be used to calculate and analyze the characteristics of electronic device-based GNRs. The effective mass of the electrons in the GNRs can be determined by applying an energy-dependent electron effective mass relation. This equation has additionally been accustomed to describing the characteristics of electronic devices, such as GNR p–n junction[16] and GNR-TFET for low power device application[17–20].

To calculate the tunneling current in the GNR-TFET, some researchers have applied the self-consistent method to determine the potential profile by solving the Poisson's equation paired with Schrödinger's equation. They then determine the transmittance by implementing the non-equilibrium Green's function formalism[17–19] and the WKB approach[20]. This paper reports the tunneling current in GNR-TFET calculated under the Dirac-like equation. A self-consistent solution of Dirac-like equation coupled with Poisson's equation is used to determine the potential profile in GNR-TFET. The transfer matrix method (TMM) has been applied to calculate the transmittance and using the Landauer Formula to compute the tunneling current. The tunneling current has been computed by implementing the TMM[21, 22], and it is suggested that the tunneling current that was calculated using the TMM is better than what has been done using the WKB[23]. These results are compared to those obtained under the Schrödinger equation with the same procedures as Dirac-like equation. The effect of gate

Correspondence to: E Suhendi, endis@upi.edu
Received 31 JANUARY 2019; Revised 21 MARCH 2019.

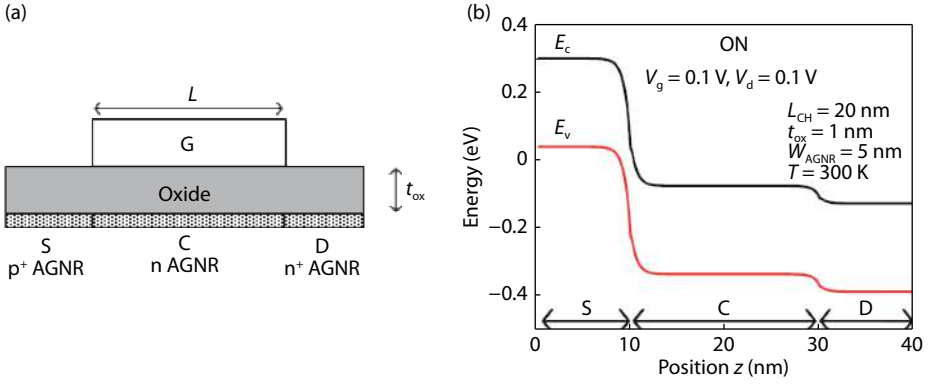

Fig. 1. (Color online) (a) The device structure of the n-channel GNR-TFET. (b) The conduction band of the GNR-TFET after self-consistency achieved.

voltage, drain voltage, width of GNR, oxide thickness, and temperature on the tunneling current in GNR-TFET is presented and compared for both calculations.

2. Theoretical model

Fig. 1(a) depicts the device structure of the n-channel GNR. We used the armchair graphene nanoribbons (AGNR) type and it is doped to be p+, n, and n+ which used as source, channel and drain, respectively. By solving the Dirac-like Hamilton equation, the Poisson's equation to consider self-consistently, the potential profile of GNR-TFET was determined. The z-direction was claimed as the finite difference method that was used to discretize the Poisson's equation and the Dirac-like Hamiltonian along the carrier transport direction,

$$H = v_{\mathrm{F}}\begin{bmatrix} 0 & -i\hbar\partial_z - \hbar\partial_x \\ -i\hbar\partial_z + \hbar\partial_x & 0 \end{bmatrix}. \tag{1}$$

From this equation, it can be seen that $\hbar$ is the reduced Planck constant and v_{F} is defined as the Fermi velocity. In this calculation, we need a guess potential as an initial value. The solution of the Poisson's equation uses the surface potential method[24] applied as a guess potential. The potentials at drain V_{d} and gate V_{g} are fixed. The iteration process between Poisson's equation and Dirac-like equation continues until self-consistency is reached. Fig. 1(b) presents the conduction band of GNR-TFET calculated using the self-consistent method.

The wave function solutions in each region are obtained by applying Eq. (1) to the electron wave function ψ,

$$\begin{aligned}
\psi_1 &= \frac{1}{\sqrt{2}}\begin{pmatrix} 1 \\ \frac{|E-V_1|}{E-V_1}\mathrm{e}^{i\theta_1} \end{pmatrix}\mathrm{e}^{ik_1 z + ik_{\mathrm{n}}x} + \frac{B_1}{\sqrt{2}}\begin{pmatrix} 1 \\ -\frac{|E-V_1|}{E-V_1}\mathrm{e}^{-i\theta_1} \end{pmatrix}\mathrm{e}^{-ik_1 z + ik_n x}, & z \leqslant 0 \\
\psi_{\mathrm{S,C,D}} &= \frac{A_{\mathrm{S,C,D}}}{\sqrt{2}}\begin{pmatrix} 1 \\ \frac{|E-V_{\mathrm{S,C,D}}|}{E-V_{\mathrm{S,C,D}}}\mathrm{e}^{i\theta_{\mathrm{SCD}}} \end{pmatrix}\mathrm{e}^{ik_{\mathrm{SCD}} z + ik_n x} + \frac{B_{\mathrm{S,C,D}}}{\sqrt{2}}\begin{pmatrix} 1 \\ -\frac{|E-V_{\mathrm{S,C,D}}|}{E-V_{\mathrm{S,C,D}}}\mathrm{e}^{-i\theta_{\mathrm{SCD}}} \end{pmatrix}\mathrm{e}^{-ik_{\mathrm{SCD}} z + ik_{\mathrm{n}}x} & 0 < z \leqslant 2L \\
\psi_2 &= \frac{A_2}{\sqrt{2}}\begin{pmatrix} 1 \\ \frac{|E-V_2|}{E-V_2}\mathrm{e}^{i\theta_2} \end{pmatrix}\mathrm{e}^{-ik_2 z + ik_{\mathrm{n}}x} & z > 2L,
\end{aligned} \tag{2}$$

where B_1, A_{S}, B_{S}, A_{C}, B_{C}, A_{D}, B_{D} and A_2 are constants, V is the potential energy, L is the channel length (the source length = the drain length = L/2), $k_{1,\mathrm{S,C,D},2} = \sqrt{\left(E - V_{1,\mathrm{S,C,D},2}\right)^2/\left(\hbar^2 v_{\mathrm{F}}^2\right) - k_{\mathrm{n}}^2}$, k_{n} is the transverse momentum, and $\theta_{1,\mathrm{S,C,D},2} = \tan^{-1}(k_{\mathrm{n}}/k_{1,\mathrm{S,C,D},2})$. Indices S, C, and D suggest the domain in source, channel, and drain in sequence. The transmittance is calculated using the TMM following the method in Refs [10, 14, 21–23]. The acquired transmittance is later applied to compute the Dirac electron tunneling current using Landauer Formula;

$$I_{\mathrm{d}} = \frac{2g_{\mathrm{v}}e}{h}\int_{E_1}^{E_2}\left[f_{\mathrm{S}}(E) - f_{\mathrm{D}}(E)\right]T(E)\mathrm{d}E, \tag{3}$$

where $f_{\mathrm{S}}(E)$ and $f_{\mathrm{D}}(E)$ are the Fermi-Dirac energy distribution functions for electrons in the source and the drain, respectively, g_{v} is the degeneration of GNR ($g_{\mathrm{v}} = 1$), h is the Planck constant, E_1 and E_2 are limit for energy integration and $T(E)$ is the electron transmittance. The same procedure was also performed on Schrödinger's equation.

3. Calculated result and discussion

The tunneling currents (I_{d}) as a function of drain voltage (V_{d}) for various gate voltages (V_{g}) calculated by using Dirac-like equation and Schrödinger equation are depicted in Fig. 2(a). The AGNRs width, channel length L, the insulator (oxide thickness) t_{ox}, and the temperature are 5 nm, 20 nm, 1 nm, and 300 K, respectively. The tunneling currents calculated by both equations indicate the same characteristics and the device shows the metal–oxide–semiconductor field-effect transistor (MOSFET) type behavior. It can be seen from the figures that the tunneling currents initially escalate with the drain voltage and they are then able to saturate. If the drain voltage increased continuously with the gate voltage fixed, the number of electrons that tunnel has not increased because the valence band at source and the conduction band in channel does not change with the increase of drain voltage. In this case, the current relatively constant and saturation occurs. Fig. 2(b) reports the tunneling currents (I_{d}) as a function of gate voltage for variety

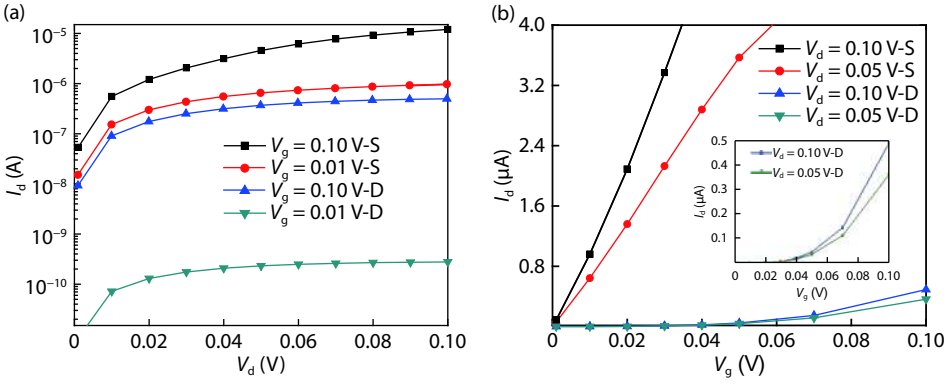

Fig. 2. (Color online) (a) The tunneling currents as a function of drain voltage for various gate voltages, (b) The tunneling currents as a function of gate voltage for various drain voltages.

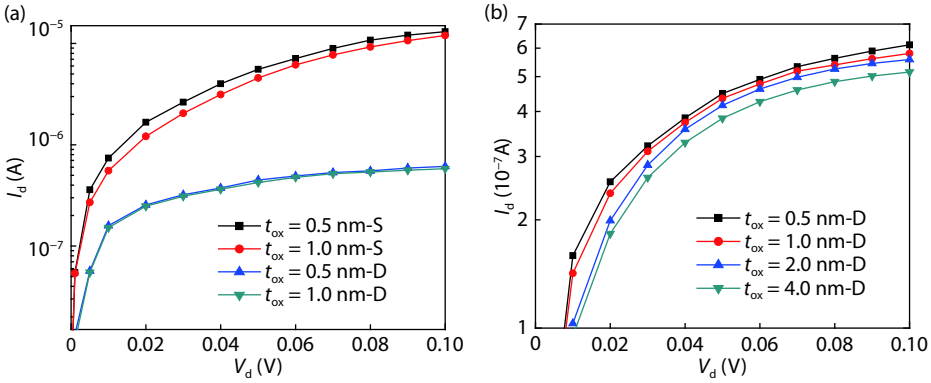

Fig. 3. (Color online) (a) The tunneling currents as a function of drain voltage for various oxide thickness for Schrödinger and Dirac-like equation, (b) The tunneling currents as a function of drain voltage for various oxide thickness for Dirac-like equation.

of drain voltages. Furthermore, the tunneling current goes up with the gate voltage. While the gate voltage is added, the conduction band in channel is reduced, so the valence band in source is higher than the conduction band in channel. Electrons stream from valence band at source to conduction band in channel. The tunneling current significantly mounts when the gate voltage escalated. In addition, the tunneling current calculated using Dirac-like equation was lower than those obtained using Schrödinger's equation.

Fig. 3(a) displays the tunneling currents as a function of drain voltage for different oxide thicknesses based on Schrödinger and Dirac-like equation. We used the gate voltage 0.1 V and the same parameters as in the other examples. From this figure, it can be inferred that the tunneling current calculated using Dirac-like equation was lower than those obtained using Schrödinger equation. There are significant differences between the tunneling currents that were calculated by using the Dirac-like equation and the Schrödinger equations for the gate voltage 0.1 V. The tunneling current as a function of the drain voltage for diverse oxide thicknesses based on Dirac-like equation has been presented in Fig. 3(b). The tunneling current increases as the thickness of the oxide decreases. When the oxide thickness goes down, the gate capacitance rises. For fixed gate voltage, the amounts of electrons in the channel escalate[25]. Thus, the tunneling current escalates when the drain voltage is applied. The dependence of the tunneling current on the oxide thickness has a similar characteristic to MOSFET, nanowire FET and CNT-FET[26].

Fig. 4(a) demonstrates the reliance of the tunneling current on the drain voltage for different AGNR widths. The AGNRs channel length L, the insulator (oxide thickness) t_{ox}, the temperature, and the gate voltage are 20 nm, 1 nm, 300 K, and 0.1 V, respectively. It can be seen that the tunneling current goes up as the AGNR width increases. This happens because the AGNR band-gap is inversely proportional to the AGNR width[5, 6]. The AGNR band-gap fell when the AGNR width increased. Consequently, more electrons entered the conduction band and the tunneling current increases. It is also found that the tunneling current calculated using Dirac-like equation is lower than that obtained using Schrödinger equation. The tunneling current differences calculated using both equations decrease as the AGNR width increases. The reliance of the tunneling current on the gate voltage for various temperatures is shown in Fig. 4(b). It was taken that the drain voltage is 0.1 V. Both calculations show that the tunneling current goes down as the temperature increase. The tunneling current is influenced by electron mobility. In this material, electron mobility is very high and it changes as the temperature changes. Electron mobility decreases when temperature increases[27, 28]. This happens because at higher temperatures, the lattice vibrations increase and this results in the probability of electrons being scattered as the lattice gets bigger. So that when the temperature grows, the electron mobility decreases[29].

The results that we have obtained suggest that the tunneling current from the calculation using Dirac-like equation is always smaller than the use of Schrödinger's equation. It is as-

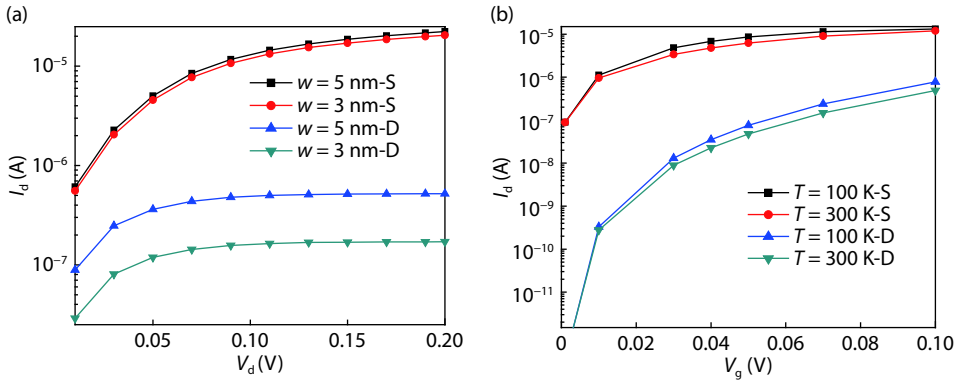

Fig. 4. (Color online) (a) The tunneling currents as a function of drain voltage for various AGNR widths. (b) The tunneling currents as a function of gate voltage for various temperatures.

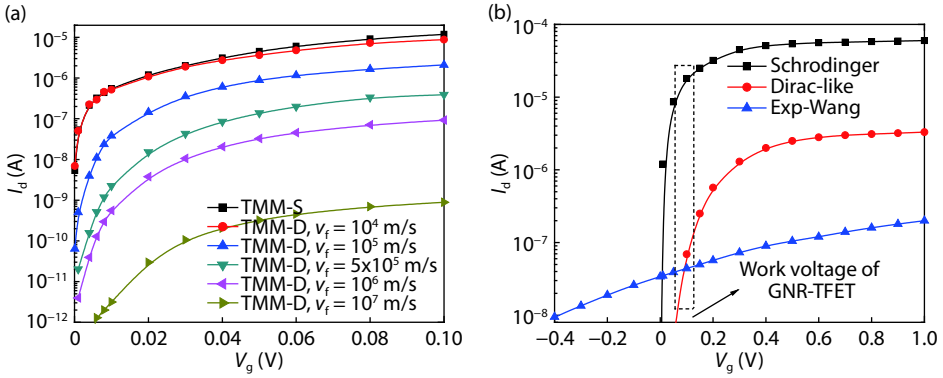

Fig. 5. (Color online) (a) Characteristics of tunneling currents on gate voltages resulting from the calculation of Dirac-like equations for variations in Fermi velocity (b) Comparison of tunneling current calculated by Schrödinger equation, Dirac-like equation and an experiment by Wang, 2008.

sumed that the Fermi velocity and the effective mass of electrons are the contributing factors because they distinguish the use of Dirac-like and Schrödinger's equations. The effect of Fermi velocity on the tunneling current characteristics is shown in Fig. 5(a). We applied Dirac-like equations in calculating the tunneling current by taking the Fermi velocity of 10^6 m/s. This value is greater than the electron Fermi velocity in other materials, such as metal and semiconductors, with a range of values 10^4–10^5 m/s. The growing electron Fermi velocity results in smaller tunneling currents, while for the electron Fermi velocity it gets smaller, and the tunneling current that was produced by the AGNR-TFET gets bigger. When the electron Fermi velocity is 10^4 m/s (red line), the tunneling current calculated using a Dirac-like equation is almost the same as the tunneling current calculated using Schrödinger's equation. The difference in the tunneling current may also be due to the different approximation of the two equations. This result explains the difference in the tunneling current resulting from the calculations using Dirac-like equation and Schrödinger's equation.

To clarify the results of this calculation, we compared the modeling data with experimental data. For comparison, we use the result of the experiment reported by Wang *et al.*, 2008[30]. The comparison of the tunneling current characteristic of the modeling and experimental result is shown in Fig. 5(b). The length and width of the AGNR used were 2 and 267 nm, respectively; the drain voltage given was 0.1 V; and the experiment was carried out at room temperature. The experimental data is not exactly the same as the modeling data but the tendency of both has the same pattern. The tunneling current increases with increasing gate voltage. The tunneling current of the experimental result is smaller than the tunneling current from the modeling results. At a gate voltage of 1 V, the difference in the Schrödinger tunneling current with the experimental result is quite large (almost three orders of magnitude), while the difference in Dirac-like tunneling current with the experimental result is smaller (one order of magnitude). At a gate voltage of 0.1 V, which is the working voltage of the GNR-TFET device, the difference in the tunneling current between the experi mental and the calculation of the Dirac-like equation falls (same order of magnitude). In the experimental device, the source and drain use metal while the channel uses AGNR. When metals are connected to AGNR, a barrier potential exists in the form of a Schottky barrier potential, which is about half the GNR bandgap[31]. The width of the AGNR used is 2 nm so that the band gap energy is around 0.69 eV and the Schottky barrier is around 0.34 eV. Whereas in the modeled AGNR-TFET device, the maximum potential barrier is the built-in potential, which is about 0.31 eV[20, 29]. The difference in potential maximum barriers causes differences in tunneling currents in both the experiment and modeling results.

Based on the results of our calculations, we suggest that the calculation method used to model a real device depends on the mobility of carrier (electrons and holes) in the material. A Dirac-like equation (relativistic) can be used to analyze the electron transport process in graphene because the charge carriers in graphene resemble relativistic particles with zero rest mass and effective speed of around $c/300$[1, 9], where c is the speed of light in a vacuum. As a result, charge carrier mobility

in graphene is very high at around 230 000 $cm^2V^{-1}s^{-1}$ at 5 K[27] and 185 000 $cm^2V^{-1}s^{-1}$ at 100 K[28]. The value of charge carrier mobility in this material is about 100 times greater than the value of charge carrier mobility in silicon material. Meanwhile, Schrödinger's equation is used to analyze electron transport in semiconductors and metals (nonrelativistic particle) because electron mobility in the material is not as large as electron mobility in graphene.

4. Conclusion

In this paper, we modeled the tunneling current in graphene nanoribbon tunnel field effect transistor (GNR-TFET). The potential profile of GNR-TFET is calculated and found to be self-consistent between the Dirac-like equation and Poisson's equation, and also Schrödinger's equation and Poisson's equation as a comparison. The tunneling current and the electron transmittance are derived by implementing the transfer matrix method (TMM). For comparison, the tunneling current is also calculated using the Schrödinger equation. It is found that the tunneling current increases with the drain voltage and it achieves saturation by applying the calculation of both equations. It has also been found that the AGNR width, the oxide thickness, and the temperature all influence the performance of the GNR-TFET. The tunneling currents increase as the thickness of the oxide decreases and it increases as the AGNR width increases. The tunneling current differences calculated using both equations decrease as the AGNR width increases. Raising the temperatures will decrease the tunneling current. In addition, the tunneling current calculated using Dirac-like equation is lower than those obtained using Schrödinger's equation. The use of the Dirac-like equation for the Fermi velocity 10^4 m/s yields a tunneling current that is close to the result calculated with Schrodinger's equation.

Acknowledgements

This work was supported by Hibah Penelitian Berbasis Kompetensi 2018 RISTEKDIKTI Republic of Indonesia.

References

[1] Novoselov K S, Geim A K, Morozov S V, et al. Electric field effect in atomically thin carbon films. Science, 2004, 306, 666
[2] Berger C, Song Z, Li X, et al. Electronic confinement and coherence in patterned epitaxial graphene. Science, 2006, 312, 1191
[3] Jena D, Fang T, Zhang Q, et al. Zener tunneling in semiconducting nanotube and graphene nanoribbon p–n junctions. Appl Phys Lett, 2008, 93, 112106
[4] Yansen W, Abdullah M, Khairurrijal. Application of airy function approach to model electron tunneling in graphene nanoribbon-based P–N junction diodes. Journal Nanosains & Nanoteknologi, 2010, 3, 18
[5] Brey L, Fertig H A. Electronic states of graphene nanoribbons. Phys Rev, 2006, B73, 235411
[6] Son Y W, Cohen M L, Loui S G. Energy gaps in graphene nanoribbons. Phys Rev Lett, 2006, 97, 216803
[7] Huang B, Yan Q, Zhou G, et al. Making a field effect transistor on a single graphene nanoribbon by selective doping. Appl Phys Lett, 2007, 91, 253122
[8] Knoch J, Appenzeller J. Tunneling phenomena in carbon nanotube field-effect transistors. Phys. Status Solidi A, 2008, 205, 679
[9] Katsnelson M I, Novoselov K S, Geim A K. Chiral tunneling and the Klein paradox in graphene. Nat Phys, 2006, 2, 620
[10] Suhendi E, Syariati R, Noor F A, et al. Simulation of Dirac tunneling current of an armchair graphene nanoribbon-based p–n junction using a transfer matrix method. Adv Mater Res, 2014, 974, 205
[11] Hung Nguyen V, Bournel A, Dollfus P. Large peak-to-valley ratio of negative-differential-conductance in graphene p–n junctions. J Appl Phys, 2011, 109, 093706
[12] Nam Do P, Dollfus P. Negative differential resistance in zigzag-edge graphene nanoribbon junction. J Appl Phys, 2010, 107, 063705
[13] Xu X, Xu G, Cao J. Electron tunneling through a trapezoidal barrier in graphene. Jpn J Appl Phys, 2010, 49, 085201
[14] Suhendi E, Syariati R, Noor F A, et al. Modeling of Dirac electron tunneling current in bipolar transistor based on armchair graphene nanoribbon using a transfer matrix method. Adv Comput Sci Res, 2015, 5, 164
[15] Chauhan J, Guo J. Assessment of high-frequency performance limits of graphene field-effect transistors. Nano Res, 2011, 4(6), 571
[16] Mukherjee U, Banerjee S, Sarkar R, et al. Single quantum well p–n junction diode based on graphene nanoribbon. Graphene, 2015, 3(1), 6
[17] Khatami Y, Kang J, Banerjee K. Graphene nanoribbon based negative resistance device for ultra-low voltage digital logic applications. App Phys Lett, 2013, 102, 043114
[18] Noei M, Moradinasab M, Fathipour M. A computational study of ballistic graphene nanoribbon field effect transistors. Phys E, 2012, 44, 1780
[19] Yang X, Chauhan J, Guo J, et al. Graphene tunneling FET and its applications in low-power circuit design. Proc of the 20th symposium on Great lakes symposium on VLSI, 2010, 263
[20] Zhang Q, Fang T, Xing H, et al. Graphene nanoribbon tunnel transistors. Electron Device Lett, 2008, 29(12), 1344
[21] Abdolkader T M, Hassan M H, Fikry W. Solution of Schrödinger equation in double-gate MOSFETs using transfer matrix method. Electron Lett, 2004, 40(20), 20
[22] Noor F A, Abdullah M, Sukirno, et al. Comparison of electron transmittances and tunneling currents in an anisotropic $TiN_x/HfO_2/SiO_2$/p-Si(100) metal–oxide–semiconductor (MOS) capacitor calculated using exponential- and airy-wavefunction approaches and a transfer matrix method. J Semicond, 2010, 31(12), 124002
[23] Shangguan W Z, Zhou X, Chiah S B, et al. Compact gate-current model based on transfer-matrix method. J Appl Phys, 2005, 97, 123709
[24] Terrill K W, Hu C, Ko P K. An analytical model for the channel electric field in MOSFETs with graded-drain structures. IEEE Electron Device Lett, 1984, 5(11), 440
[25] Ferry D K, Goodnick S M, Bird J. Transport in nanostructures. Cambrige: Cambridge University Press, 2009
[26] Tiwari M, Sharma K K, Rawat L S, et al. Impact of oxide thickness on gate capacitance, drain current and transconductance – a comprehensive analysis on MOSFET, nanowire FET and CNTFET devices. Int J Res Emerg Sci Technol, 2015, 2, 73
[27] Bolotin K I, Sikes K J, Jiang, Z, et al. Ultrahigh electron mobility in suspended graphene. Solid State Commun, 2008, 146, 351
[28] Du X, Skachko I, Barker A, et al. Approaching ballistic transport in suspended graphene. Nature Nanotechnol, 2008, 3, 491
[29] Sze S M. Semiconductor devices, physics and technology. New Jersey: John Wiley & Sons, 1985
[30] Wang X, Ouyang Y, Li X, et al. Room-temperature all-semiconducting sub-10-nm graphene nanoribbon field-effect transistors. Phys Rev Lett, 2008, 100(20), 206803
[31] Jimenez D. A current-voltage model for Schottky-barrier graphene based transistors. Nanotechnology, 2008, 19, 345204